Optimisation of an Electrochemical Impedance Spectroscopy aptasensor by exploiting Quartz Crystal Microbalance with Dissipation Signals

Nello Formisano[1], Pawan Jolly[1], Nikhil Bhalla[1], Mary Cromhout[2], Shane P. Flanagan[2], Ronen Fogel[2], Janice L. Limson[2], Pedro Estrela[1,*]

[1]Department of Electronic & Electrical Engineering, University of Bath, Bath BA2 7AY, United Kingdom; Emails: N.Formisano@bath.ac.uk (N.F.), P.Jolly@bath.ac.uk (P.J.), N.Bhalla@bath.ac.uk (N.B.), P.Estrela@bath.ac.uk (P.E.)

[2]Department Biochemistry, Microbiology and Biotechnology, Rhodes University, P.O. Box 94, Grahamstown, South Africa; Emails: R.Fogel@ru.ac.za (R.F.), J.Limson@ru.ac.za (J.L.L.)

*Corresponding author: Department of Electronic & Electrical Engineering, University of Bath, Claverton Down, Bath, BA2 7AY, United Kingdom
E-mail: P.Estrela@bath.ac.uk
Phone: +44-1225-386324

Abstract

The response of an Electrochemical Impedance Spectroscopy (EIS) sensor using DNA aptamers is affected by many factors such as DNA density, charge and conformational changes upon DNA-target binding and buffer conditions. We report here for the first time on the optimisation of an EIS aptamer-based sensor by using Quartz Crystal Microbalance with Dissipation mode (QCM-D). As a case study we employed a DNA aptamer against Prostate Specific Antigen (PSA). PSA detection was achieved by functionalizing the gold sensor surface via thiol chemistry with different ratios of thiolated-DNA aptamer and 6-mercapto-1-hexanol (MCH) used as spacer molecules. PSA binding efficiency can be monitored by measuring QCM-D signals which not only provides information about the mass of PSA bound on the sensor surface but also crucial information about the aptamer conformation and layer hydration.

Data generated through QCM-D analysis provided the optimal conditions in terms of aptamer/MCH ratio to maximize the PSA binding. The ratio of 1:200 for DNA aptamer/spacer molecule was found to be optimal for ensuring maximum PSA binding. However, this study showed how a maximum analyte binding does not necessarily correspond to a maximum EIS response, which revealed to be enhanced if a ratio of 1:100 for DNA aptamer/spacer molecule was used. Moreover, by monitoring the QCM-D signal, for the first time a value of the dissociation constant (K_d), equal to 37 nM, was found for the PSA DNA aptamer towards its target. The combination of QCM-D with EIS techniques provide further insight into the effects of mass loading and charge effects that govern the response of an EIS aptasensor, serving as a valuable support for future EIS aptamer-based applications.

1. Introduction

A global demand for cost-effective, reliable and rapid tools for the early detection of disease markers has led to an intensive study of label-free biosensors in the last decade as point-of-care diagnostic platforms. Label-free sensors represent the new frontier for DNA-based detection. The lack of labelling processes lowers their individual expense and responses are more rapid when compared to enzyme or fluorescent-labelled assays (Keighley et al., 2008). Furthermore, label-free DNA-based sensors can be widely employed in achieving high genosensor sensitivity for genetic disease and forensic detection applications. One of the most promising label-free measurement techniques for DNA applications is Electrochemical Impedance Spectroscopy (EIS). EIS measures changes in electrode impedance upon target recognition, with reported sensitivities down to attomolar ranges (Bertok et al., 2013).

Antibodies currently represent the gold standard in modern biosensing platforms for protein detection. However, antibodies are affected by some disadvantages, particular to their *in vivo* production. *In vivo* conditions hamper freedom in manipulating processes and can lead to significant batch-to-batch variability (Keefe et al., 2010). Moreover, the shelf lives of antibodies can prevent their effective integration into biosensor platforms (McKeague et al., 2011). Alternatively, DNA aptamers are produced by *in vitro* selection of functional nucleic acids through a process called Systematic Evolution of Ligands by Exponential enrichment (SELEX) (Stoltenburg et al., 2007). Unlike antibodies, DNA aptamers can be inexpensively synthesized and chemically modified with high purity and reproducibility. Furthermore, they are small in size, chemically stable and can target not only small molecules but also large proteins and cells, while exhibiting affinities and sensitivities similar to antibodies (Song et al., 2008). Their continued generation and investigation is consistently grouped around their application as biorecognition agents in diagnostic and therapeutic technologies.

In this study, we investigated the correlations between EIS and QCM-D signals of an aptasensor, using the detection of prostate-specific antigen (PSA) with a DNA aptamer as a case study. PSA is a 33-34 kDa glycoprotein produced by the prostate, a gland which liquefies semen in order to increase sperm mobility. Altered levels of PSA in blood above the cut off level of 120 pM might be associated

with prostate cancer (PCa) (Gilgunn et al., 2013). PCa is the second worldwide leading cause of cancer-related mortality amongst men (Ferlay et al., 2013). The slow progression, coupled with the lack of symptoms during the first stages of the disease, often leads to a late diagnosis of the tumour, hampering the efficacy of medical interventions. At present, the most reliable screening consists of histological analysis performed by collecting sample tissues through a biopsy (Lilja et al., 2008; Gilgunn et al., 2013). However, such procedure can produce several inconveniences (Basch et al., 2012) such as infection complications. The decision of whether or not performing a biopsy is largely based on digital rectal examination and the measurement of PSA blood levels.

Current label-free detection systems for PSA involve mostly antibody-based electrode fabrication. Arya & Bhansali (2012) proposed a sensing system where gold electrodes are functionalized with a cysteamine self-assembled monolayer (SAM) by using conventional EDC/NHS chemistry. Li et al. (2005) proposed a combined use of In_2O_3 nanowires and p-type carbon nanotubes, where antibodies are immobilized through succinimidyl linking molecules. Chiriacò et al. (2013) developed an EIS sensor for both total and free PSA detection on gold electrodes by exploiting two different antibodies and using a SAM made of 11-mercaptoundecanoic acid and 2-mercaptoethanol and EDC/NHS chemistry.

At present, very few studies on PSA detection using an aptasensor have been reported (Jolly et al., 2015a), all of them using the sequence developed by Savory et al. (2010). Liu et al. (2012) performed Differential Pulse Voltammetry (DPV) measurements on graphite electrode with gold nanoparticles encapsulated by graphitized mesoporous carbon, exploiting biotinylated-aptamer/streptavidin coupling, achieving a limit of detection (LOD) of 7 pM with a dynamic range from 7 pM to 6 nM. Cha et al. (2014) reported on a chemiluminescent resonance energy transfer aptasensor for PSA with a LOD of 30 pM. A chemiluminescent aptasensor able to remove impurities that hamper PSA detection in human serum with sensitivity comparable to enzyme immunoassays was developed by Choi & Lee (2013). A detection limit as low as 5 aM was achieved by Ma et al. (2014) employing a sensor based on surface enhanced Raman scattering in serum samples. Jolly et al. (2015b), instead, reported on an EIS aptamer-based aptasensor that makes use of the anti-fouling properties of sulfo-betaine molecules

for the formation of the SAM. Chen et al. (2012) instead, proposed an optical method of detection in the range 4 pM to 3 nM with LOD of ~1 pM, based on a resonance light-scattering (RLS) and gold nanoparticles assay where the changes in aptamer conformation upon PSA recognition is exploited.

Although EIS aptasensors are extremely promising, a careful optimization of the factors that can cause undesired signal changes is required. It is known that the immobilised DNA density and the hydration, charge and conformation of the biomolecular sensing layer can affect the EIS response (Radi & O'Sullivan, 2006). Moreover, the amount of DNA aptamer on the secondary structure (i.e. upon antigen binding, which conformation requires a higher energy state) also depends on steric hindrance effects as well as on the DNA density which directly affects the electrostatic interactions between DNAs. The support of Quartz Crystal Microbalance with Dissipation mode (QCM-D) can provide valuable information on the status of the biolayer, such as the amount of bound mass and the viscoelastic properties of the film. The QCM-D system allows real time measurements of the mass bound at the interface of a gold-coated quartz crystal, which can inform certain properties of immobilised biomolecules for sensing purposes (Fogel et al., 2007; Fogel & Limson, 2011). The measurements are carried out by monitoring resonance frequency and energy dissipation changes happening at the interface of the oscillator when this is excited at its fundamental resonance frequency or integer odd multiples. Here, we (i) compare EIS with QCM-D signals in order to obtain the best conditions that maximize the response of an EIS aptasensor using, as a case study, PSA as a target analyte and (ii) we provide further understanding of the EIS response for aptamer-based sensors which can be used as valuable support for future applications.

The principle of detection of the aptasensor is described in figure 1. A DNA aptamer raised against PSA (Savory et al., 2010) was used to specifically bind the target. Since functionalization of the electrodes with mixed SAMs fosters a better SAM formation for electrochemical applications (Steel et al., 1998), in order to increase the performance of the biosensor, a mixed SAM was employed where the thiolated DNA served as capture probe and MCH was chosen as a spacer molecule. MCH was included in order to alter the lateral density of thiolated DNA on the surface; this was to passivate the gold surface and reduce non-specific binding as well as minimise steric hindrance and facilitate the

charge transfer during the EIS measurements (Keighley et al., 2008). Although gold-sulphur bonds happen relatively quickly, a longer exposure (such as 16 hours) with the alkanethiols solution leads to the formation of a well-organized SAM structure which ensures a better approaching of the ferri/ferrocyanide redox couples $[Fe(CN)_6]^{3-/4-}$ to the electrode surface, thereby yielding a more reliable EIS recording (Love et al., 2005).

Since aptamer conformation can be very sensitive to the environment where aptamers are employed (Pestourie et al., 2006; Radi & O'Sullivan, 2006), important conditions such as aptamer/MCH ratio used for the sensor surface functionalization were investigated in order to maximize the biosensor efficiency. Similarly, EIS signals can be affected by different factors such as the conformational modifications of the aptamer structure during aptamer-antigen recognition, which leads to the redistribution of the coverage charges and subsequent alteration of the impedance spectrum. However, the conformational changes are not anticipated to affect the QCM-D response as significantly, since the oscillating frequency change signal is more dependent on the alteration of total mass bound on the crystal surface and alterations in the hydration level of the bound layer, induced by the protein binding.

2. Material and methods

2.1. Reagents

Thiolated PSA aptamer (5'-HS-$(CH_2)_6$-TTT TTA ATT AAA GCT CGC CAT CAA ATA GCT TT-3'), 6-Mercapto-1-Hexanol (MCH), Human Serum Albumin (HSA), potassium phosphate, monobasic solution 1 M, potassium phosphate dibasic solution 1 M, potassium sulphate, potassium hexacyanoferrate (III), potassium hexacyanoferrate (II) trihydrate, Tris-HCl, ethylenediaminetetraacetic acid (EDTA), magnesium chloride, sodium chloride and potassium chloride were obtained from Sigma-Aldrich (UK). Ethanol was purchased from Fisher Scientific (UK). PSA from human seminal fluid in PBS, pH 7.4, 0.1% NaN_3, purity ≥98% by SDS-PAGE (product number 539831) was purchased from Merck Chemicals Ltd (UK). Ultrapure water

(18.2 MΩ cm) was used for all the aqueous solutions (Millipore, USA). All other reagents were of analytical grade.

2.2. Immobilization procedure/ sensor fabrication

Gold electrodes used for QCM-D and EIS measurements were incubated for 16 hours at room temperature, suspended in a 150 µl mixture of thiolated DNA aptamer (HS-$(CH_2)_6$-ssDNA) and MCH. Prior to mixing with DNA aptamer, MCH was initially diluted in ethanol to form a stock solution of 100 mM and then in measurement buffer and mixed with the thiolated aptamer. Various ratios of MCH to aptamer were combined to reach a final concentration of 100 µM of total thiol. 1:50, 1:100, 1:200 and 1:500 ratios of aptamer:MCH were investigated in this study. In order to activate the DNA aptamer, the DNA sample was heated for 10 min at 95 °C and rapidly cooled down to 0 °C before being mixed to MCH for the sensor functionalization. Target detection was tested by adding 11, 22, 44, 89, 200, and 400 nM of PSA.

2.3. EIS system

A µAUTOLAB III / FRA2 potentiostat (Metrohm, Netherlands) was used to perform impedance measurements in a three-electrode cell with a Hg/Hg_2SO_4 reference electrode (BASi, USA) and a platinum wire counter electrode (ALS, Japan). Gold electrodes of 1.0 mm radius were used as working electrodes (CH Instruments, USA); prior their use, the electrodes were sonicated for 10 min in ethanol and then mechanically polished for 5 min on polishing pads by using 50 nm alumina slurry (Buehler). A further 5 min sonication in ultrapure water was carried out and finally the electrodes were electrochemically polished by performing 50 scans of the potential between -0.05 V and +1.10 V *versus* Hg/Hg_2SO_4 in 0.5 M H_2SO_4. All the steps were followed by a thorough rinsing with ultrapure water.

Impedance measurements were recorded in 0.1 M phosphate buffer, 0.1 M KCl, 10 mM ferri/ferrocyanide $[Fe(CN)_6]^{3-/4-}$ (EIS measurement buffer), scanning 61 frequencies between 100 KHz

and 0.1 Hz applying a 10 mV a.c. voltage superimposed to the formal potential of the $[Fe(CN)_6]^{3-/4-}$ redox couple (0.190 V *versus* Hg/Hg_2SO_4). All the measurements were carried out in triplicate, values reported in this study are the mean of replicates. Reported errors are standard deviations from the mean. EIS recordings were repeated every 30 min prior to the interaction with PSA until the signal was stable for two consecutive measurements. The impedance of the electrochemical interface was modelled with a Randles equivalent circuit where the double layer capacitance (C_{dl}) has been replaced by a constant phase element (CPE) in order to obtain a better estimation of the electrochemical double layer of the real system (Macdonald, 1984) (inset Fig. 2).

The negative charge of the DNA aptamer produces an electrostatic barrier to the negatively charged redox marker $[Fe(CN)_6]^{3-/4-}$, which hinders the charge transfer processes between the redox marker in solution and the electrode. For this reason, a higher aptamer density on the electrode surface results in higher values of charge transfer resistance (R_{ct}). When PSA binds to the aptamer, a conformational change of the DNA strand occurs with a consequent modification of the layer structure and of possible screening of the DNA charges. As a result, the binding of the analyte to the aptamer causes a change in the impedance of the system and, in particular, in R_{ct}.

2.4. Chronocoulometry

Chronocoulometry of aptamer-modified electrodes was performed in order to estimate the DNA aptamer density on the electrode surface for different ratios of MCH/aptamer. The measurements were performed with a μAUTOLAB III potentiostat in a three electrode system using 10 mM Tris buffer pH 7.4, both in the absence and presence of 100 μM of hexaammineruthenium(III) chloride, $Ru(NH_3)_6^{3+}$. The potential was stepped from −0.3 V, where the potential was held for 200 ms, to -0.8 V *versus* $Hg/HgSO_4$ and held at this value for 500 ms while the resulting currents were recorded. The values of aptamer molecules per electrode area were calculated using a modified Cottrell equation (Keighley et al, 2008).

2.5. QCM-D system

Prior to modification and subsequent testing, AT-cut 5 MHz gold coated quartz crystals (QSX301) gold-coated quartz crystals were cleaned by exposure to a solution of 5:1:1 of ultrapure water, hydrogen peroxide and ammonia preheated at 75 °C for 5 minutes. Cleaned crystals were rinsed successively with ultrapure water, ethanol and, again, ultrapure water and dried with nitrogen gas. A further step of 1 min UV/ozone exposure provided the final removal of organic contaminants before the crystals could be used for the QCM-D measurement.

Quartz crystals were mounted in titanium chambers and used with an E4 QCM-D sensor system (Q-Sense, Sweden). The chamber temperature was set at 21.2 °C. DNA immobilization, PSA binding and measurements were performed in the same buffer in which the aptamer was raised (Savory et al., 2010): 10 mM Tris HCl, 150 mM NaCl, 5 mM KCl, 5 mM $MgCl_2$, pH 7.4 (TBS buffer) with an ionic strength of 175 mM. In order to compare the amount of PSA bound on the quartz crystal for different aptamer/MCH fractions, four concentrations of PSA were tested: 0, 22, 89 and 200 nM. QCM-D analysis made use of an Ismatec peristaltic pump, set on a flow rate of 20.0 µl/min. After finding the best aptamer/MCH fraction, the biosensor detection was tested with dissolved PSA concentrations ranging between 0 and 400 nM. Sauerbrey and Voigt masses which respectively give an approximate estimation of the dry and hydrated immobilised masses were calculated, using the frequency and dissipation values generated during protein titration. For thin, rigid films the Sauerbrey equation (1) states that the shift in the resonant frequency, Δf, of a piezoelectric sensor is directly proportional to the amount of mass bound on the sensor surface, Δm (O'Sullivan & Guilbault, 1999):

$$\Delta m = \frac{C\Delta f}{n} = \frac{A\sqrt{\mu_q \rho_q}}{2nf_0^2}\Delta f \qquad (1)$$

where f_0 is the fundamental frequency of the quartz crystal (Hz), A the sensing area of the electrode (cm^2), μ_q and ρ_q are the shear modulus (2.947×10^{11} $g/s^2\,cm$) and density (2.648 g/cm^3) of the quartz crystal, respectively and n is the overtone number (n = 1, 3, 5. etc). $C = 17.7$ ng/ Hz cm^2 is the mass sensitivity constant for the AT-cut 5 MHz quartz crystal used in this study.

For bound biomolecule layers, a percentage as high as 95% of water can be entrapped in the adsorbed film. When water is coupled to the biological layer, a soft and viscoelastic film can form and additional dampening of the quartz oscillator occurs causing an overestimation of the mass if only the Sauerbrey equation is used to model the system (Höök et al., 2001). By measuring both the frequency and dissipation factor of the quartz crystal, QCM-D can overcome this limitation providing a more accurate estimation of the mass of the layer (Fogel & Limson, 2011). The dissipation factor measures the ratio between the lost energy and the stored energy from the system during one oscillation cycle. The compensation of the viscous energy losses is achieved using the Voigt model (Voinova et al., 1999; Dutta et al., 2008; Höök et al., 2001). The Voigt model was fitted using the QTools software (LOT-Oriel AG, Germany) by setting a film density of 1050 kg/m^3 and fluid viscosity of 0.001 kg/m s. From these bound mass responses, the dissociation constant of the PSA-immobilised aptamer complex was calculated

3. Results and discussion

3.1. DNA-aptamer/MCH ratio

In order to control the aptamer density on the gold surface, the sensor functionalization was achieved by means of a mixed SAM, i.e. aptamer and MCH were mixed before performing the functionalization step. The aptamer distribution and density play a crucial role in the biosensor performance (Keighley et al., 2008). For example, electrode functionalization performed with mixed SAMs of 1:9 and 1:200 aptamer/MCH ratio yielded signal changes of 27 and 7.5 Hz, respectively. A further step of MCH backfilling provided further electrode coverage due to SAM reorganization, coverage of pinholes in the initial SAM, and lifting of any DNA lying flat on the surface due to electrostatic interactions.

Four different aptamer/MCH ratios were tested: 1:50, 1:100, 1:200 and 1:500. Preliminary results showed that lower aptamer/MCH ratios such as 1:9 produced a minor response (0.76%) in ΔR_{ct} upon addition of 300 nM PSA. The aptamer density coverage for different aptamer/MCH fraction was

analysed by performing chronocoulometry measurements (Fig. 3). These results were confirmed by EIS signals, which showed increasing values of initial R_{ct} as the ratio is decreased: 1059 ± 43 Ω, 1557 ± 50 Ω, 1634 ± 164 Ω and 1858 ± 161 Ω for 1:500, 1:200, 1:100 and 1:50 aptamer/MCH ratios, respectively, which linearly correlates with DNA aptamer density from chronocoulometry data.

In order to evaluate the performance of the biosensor, three PSA solutions with concentrations of 22, 89 and 200 nM were tested. By analysing the responses from the Voigt model, the four aptamer/MCH ratios showed different levels of hydration and of total PSA mass bound (Fig. 4). At an aptamer:MCH ratio of 1:200, an increase in PSA binding was recorded by the QCM-D system, relative to the other ratios studied. Analyzing the hydrated response, i.e. combining the dry mass response with the dissipation signal, the electrode functionalized with an aptamer/MCH ratio of 1:200 exhibited the highest response in terms of PSA binding, with an extent of pmoles/cm^2 129% higher than the electrode functionalized with a ratio of 1:50. However, a further decrease of the aptamer fraction (ratio 1:500) lowered the efficiency of the biosensor as shown in Fig. 4. The trend obtained can be explained considering the combination of two effects: the steric hindrance effect, which prevails for ratios up to 1:200, and the total number of aptamer molecules available for PSA targeting, which becomes more consistent for a lower DNA aptamer fraction. Furthermore, QCM-D revealed the difference in hydration amongst the four ratios. If we divide the amount of Voigt mass, i.e. the hydrated mass, by the Sauerbrey mass, i.e. the dry mass, we can have an indication of the hydration level for each DNA aptamer/MCH fraction analysed. Respectively, 1:50, 1:100, 1:200 and 1:500 exhibited an average hydration level across the points shown in fig. 4 of 1.01, 0.80, 1.19 and 1.37. The highest hydration level was, therefore, achieved for the 1:500 ratio. However, as shown in fig. 4, the 1:500 ratio does not guarantee enough DNA aptamer coverage in order to ensure the maximum PSA binding to the sensor surface.

3.2. Comparison of QCM-D and EIS data

In order to test the performance of the system, impedance measurements were compared for PSA concentrations between 300 fM and 300 nM for different DNA aptamer/MCH ratios (Fig. 5).

Measurements showed a general trend where the biosensor impedance moved towards smaller R_{ct} values upon increasing PSA concentrations as can be seen in the Nyquist plots in Fig. 2. It is worthwhile to highlight the negative changes in impedance signals due to PSA binding. The isoelectric point of the PSA is between 6.9 and 7.2 (Zhang et al., 1995), so its binding to the DNA aptamer is supposed to add a small increase in negative charge to the system when the biosensor is operated in the pH range between 7.0 and 7.4, which would increase the electrostatic barrier to the redox couple $[Fe(CN)_6]^{3-/4-}$, therefore increasing slightly R_{ct}. The folding of the DNA aptamer into its secondary structure upon PSA binding increases the density of charge closer to the surface and expands it to a larger geometrical area – factors which should also lead to an increase in R_{ct}. The presence of the bulky PSA molecules on the surface have an obstructing effect to the redox markers and would further hamper the electron transfer during EIS measurements. Decreases in R_{ct} upon target binding to an aptamer, although not common, have been reported in a couple of systems including PSA (Rodriguez at al., 2005; Jolly et al., 2015b) and been attributed to a partial screening of the negative charge of the DNA aptamer by PSA binding, which lowers the electrostatic barrier to the redox markers, facilitating their approach to the sensor surface. The EIS response is in fact due to the combination of all the effects mentioned: a negative shift in R_{ct} is only observed when the screening of the DNA aptamer charge caused by the protein binding is the dominant effect (Jolly et al., 2015b). Such effect was more relevant for high concentrations of PSA. The ΔR_{ct} *versus* [PSA] curves roughly follow a Hill dose response equation of the type $y = y_0 + (y_{max} - y_0)\, c^n / (k^n + c^n)$ where c is the concentration. However, no accurate values of the parameters can be extracted from the fits, presumably due to the complex dependencies of R_{ct} on the charge and mass of the biolayer.

It is observed that the maximum EIS signal is obtained for an aptamer/MCH ratio of 1:100. Moreover, the reproducibility of the EIS signals is also improved for the 1:100 aptamer/MCH ratio. The EIS signal depends not only on the total mass bound on the surface (for which a maximum signal is obtained for a 1:200 ratio as seen by the QCM-D) but also on the screening of the DNA charge, which is expected to be higher for more densely packed DNA layers. The LODs obtained from the EIS data improve as one goes from a ratio of 1:500 towards 1:200 and 1:100, where the best value was

obtained (<40 nM). However, for the 1:50 ratio there is a significant increase in the LOD. Correlating the LODs obtained from the EIS responses for different aptamer densities (inset Fig. 3), it can be seen that small changes of aptamer/thiols fraction can greatly affect the sensitivity towards the PSA detection: e.g. an increase in aptamer surface density from 1.2 to 1.5×10^{12} molecules/cm^2, leads to a significant increase in LOD. It is this fine balance between mass loading and charge effects that leads to a different optimal ratio for EIS measurements. In our previous reported work (Jolly et al., 2015b), the stability of the aptasensor with respect to repeated EIS measurements over time was studied. It was also reported the effect of changing types of buffer on the impedance signal as to make a clear point on reliable acquisition of data reflecting only binding of PSA to the aptasensor.

Figure 6A shows the QCM-D kinetic curves of frequency shift and dissipation changes for a 1:200 aptamer/MCH ratio. It can be seen how increasing concentrations of PSA added to the chamber in flow conditions follow typical association curve responses. Moreover, PSA additions enhanced the viscoelastic properties of the biofilm as shown by the dissipation response. The dissipation signal allows estimating the mass of protein bound to the aptamer with a better accuracy. This can be extremely important in particular for low concentrations of PSA where a correction as large as 10 fold was obtained when using the Voigt model as compared to the solely dry mass response. Figure 6B shows the hydrated QCM-D responses for PSA and human serum albumin (HSA) obtained with the aptamer:MCH ratio of 1:200. QCM-D data shows a hyperbolic dose-response with an affinity constant $K_d = 37$ nM for PSA. With respect to the EIS response, a concentration as high as 100 µM of HSA, which is the concentration typically found in blood, produced a shift in R_{ct} of $12 \pm 6\%$. However, unlike for PSA, the shift in R_{ct} deriving from non-specific binding of HSA is positive and, hence, easily distinguishable from PSA. The non-specific binding of proteins occurs primarily within the MCH areas, yielding an increase in R_{ct} due to a blocking effect towards the redox couple. We cannot neglect that using the biosensor in presence of both proteins, this would result in a lower efficacy towards PSA detection. However, since the aim of this study is not to develop a PSA sensor but to provide a comparative study between QCM-D and EIS signals, we leave the optimization of such an aptasensor to further studies.

4. Conclusions

In this study we investigated strategies for the optimization of an EIS aptamer-based sensor. We used a PSA-specific aptamer as a case study and monitored the total PSA mass bound by varying the binding conditions and recording QCM-D data. We found a K_d value of 37 nM for the DNA aptamer towards its PSA target. QCM-D results confirmed the importance of DNA surface coverage optimization for efficient aptamer-protein binding. In particular we found that a ratio 1:200 of aptamer:MCH provides the maximum PSA binding. However, EIS data demonstrated a higher DNA aptamer surface density (obtained for a 1:100 ratio) is required for an optimal impedimetric signal. A negative R_{ct} signal change was recorded upon targeting the DNA aptamer as a result of the screening of the aptamer charge by bound PSA. Impedimetric measurements in aptasensors depend on the balance between different factors such as the antigen binding bulk effect, surface charge, and DNA conformational changes happening upon target binding. Therefore, the DNA aptamer surface density for which maximum antigen binding occurs, is not necessarily the optimal surface density for EIS measurements. In this study we have shown a decrease in the ΔR_{ct} signal upon targeting the DNA aptamer. The decrease in R_{ct} cannot, however, be generalized for any aptamer-based sensor as the EIS signal is not only generated by the obstructing effect induced by the target binding but also by the charge and conformational redistributions that happen on the sensor surface. A direct consequence is that a maximum analyte binding, as here demonstrated, not always corresponds to a maximum signal response for an EIS sensor. Although aptamers have great potential towards the development of biosensors, aptasensors require a careful design in order to provide an acceptable binding efficiency. The results of this study can be applied to future label-free, reliable and cost effective aptamer-based sensors exploiting EIS.

Acknowledgments

NF and PE acknowledge the University of Bath for an International Researcher Mobility Award. PJ is funded by the European Commission FP7 Programme through the Marie Curie Initial Training Network “PROSENSE” (Grant No. 317420, 2012–2016).

References

Arya, S. K. & Bhansali, S. (2012). Anti-Prostate Specific Antigen (Anti-PSA) modified interdigitated microelectrode-based impedimetric biosensor for PSA detection. *Biosensors Journal, 1,* H110601. doi:10.4303/BJ/H110601

Basch, E., Oliver, T. K., Vickers, A., Thompson, I., Kantoff, P., Parnes, H., Loblaw, D. A., Roth, B., Williams, J., & Nam, R. K. (2012). Screening for prostate cancer with prostate-specific antigen testing: American Society of Clinical Oncology provisional clinical opinion. *Journal of Clinical Oncology, 30*(24), 3020–3025. doi:10.1200/JCO.2012.43.3441

Bertok, T., Sediva, A., Katrlik, J., Gemeiner, P., Mikula, M., Nosko, M., & Tkac, J. (2013). Label-free detection of glycoproteins by the lectin biosensor down to attomolar level using gold nanoparticles. *Talanta, 108,* 11–18. doi:10.1016/j.talanta.2013.02.052

Cha, T., Cho, S., Kim, Y. Y., & Lee, J. H. (2014). Rapid aptasensor capable of simply diagnosing prostate cancer. *Biosensors and Bioelectronics, 62,* 31-37. doi:10.1016/j.bios.2014.06.015

Chen, Z., Lei, Y., Chen, X., Wang, Z., & Liu, J. (2012). An aptamer based resonance light scattering assay of prostate specific antigen. *Biosensors and Bioelectronics, 36,* 35-40. doi:10.1016/j.bios.2012.03.041

Chiriacò, M. S., Primiceri, E., Montanaro, A., de Feo, F., Leone, L., Rinaldi, R., & Maruccio, G. (2013). On-chip screening for prostate cancer: an EIS microfluidic platform for contemporary detection of free and total PSA. *Analyst, 138*(18), 5404–5410. doi: 10.1039/c3an00911d

Dutta, A. K., Nayak, A., & Belfort, G. (2008). Viscoelastic properties of adsorbed and cross-linked polypeptide and protein layers at a solid-liquid interface. *Journal of Colloid and Interface Science*, *324*(1-2), 55–60. doi:10.1016/j.jcis.2008.04.065

Choi, H. K., & Lee, J. H. (2013). Role of magnetic Fe_3O_4 graphene oxide in chemiluminescent aptasensors capable of sensing tumor markers in human serum. *Analytical Methods, 5*, 6964-6968. doi:10.1039/C3AY41683F

Ferlay, J., Soerjomataram, I., Ervik, M., Dikshit, R., Eser, S., Mathers, C., Rebelo, M., Parkin, D. M., Forman, D., & Bray, F. (2013). GLOBOCAN 2012 v1.0, Cancer Incidence and Mortality Worldwide: IARC CancerBase No. 11 [Internet]. Lyon, France: International Agency for Research on Cancer. Available from: http://globocan.iarc.fr, accessed on 19/12/2014

Fogel, R., Mashazi, P., Nyokong, T & Limson, J. (2007). Critical assessment of the Quartz Crystal Microbalance with Dissipation as an analytical tool for biosensor development and fundamental studies: metallophthalocyanine - glucose oxidase biocomposite sensors. *Biosensors and Bioelectronics*, 23, 95 – 101. doi:10.1016/j.bios.2007.03.012

Fogel, R., & Limson, J. L. (2011). Probing fundamental film parameters of immobilized enzymes – towards enhanced biosensor performance. Part I – QCM-D mass and rheological measurements. *Enzyme and Microbial Technology*, *49*(2), 146–152. doi:10.1016/j.enzmictec.2011.05.011

Gilgunn, S., Conroy, P. J., Saldova, R., Rudd, P. M. & O'Kennedy, R. J. (2013). Aberrant PSA glycosylation—a sweet predictor of prostate cancer. *Nature Reviews Urology*, *10*(2), 99-107. doi: 10.1038/nrurol.2012.258

Höök, F., Kasemo, B., Nylander, T., Fant, C., Sott, K., & Elwing, H. (2001). Variations in coupled water, viscoelastic properties, and film thickness of a Mefp-1 protein film during adsorption and cross-linking: a quartz crystal microbalance with dissipation monitoring, ellipsometry, and surface plasmon resonance study. *Analytical Chemistry*, *73*(24), 5796–5804. doi: 10.1021/ac0106501

Jolly, P., Formisano, N., & Estrela, P. (2015a). DNA aptamer-based detection of prostate cancer. *Chemical Papers, 69*(1), 77-89. doi: 10.1515/chempap-2015-0025

Jolly, P., Formisano, N., Tkac, J., Kasak, P., Frost, C. G., & Estrela, P. (2015b). Label-free impedimetric aptasensor with antifouling surface chemistry: a prostate specific antigen case study. *Sensors and Actuators B, 209*, 306-312. doi: 10.1016/j.snb.2014.11.083

Keefe, A. D., Pai, S., & Ellington, A. (2010). Aptamers as therapeutics. *Nature Reviews Drug Discovery*, *9*(7), 537–550. doi:10.1038/nrd3141

Keighley, S. D., Li, P., Estrela, P., & Migliorato, P. (2008). Optimization of DNA immobilization on gold electrodes for label-free detection by electrochemical impedance spectroscopy. *Biosensors and Bioelectronics*, 23(8), 1291–1297. doi:10.1016/j.bios.2007.11.012

Li, C., Curreli, M., Lin, H., Lei, B., Ishikawa, F.N., Datar, R., Cote, R.J., Thompson, M.E., & Zhou, C. (2005). Complementary detection of prostate-specific antigen using In2O3 nanowires and carbon nanotubes. *Journal of American Chemical Society, 127(36),* 12484-12485. doi: 10.1021/ja053761g

Lilja, H., Ulmert, D., & Vickers, A. J. (2008). Prostate specific antigen and prostate cancer: Prediction, detection and monitoring. *Nature Reviews Cancer, 8,* 268–278. doi:10.1038/nrc2351

Liu, B., Lu, L. S., Hua, E. H., Jiang, S. T., & Xie, G. M. (2012). Detection of the human prostate-specific antigen using an aptasensor with gold nanoparticles encapsulated by graphitized mesoporous carbon. *Microchimica Acta, 178,* 163–170. doi: 10.1007/s00604-012-0822-5

Love, J. C., Estroff, L. A, Kriebel, J. K., Nuzzo, R. G., & Whitesides, G. M. (2005). Self-assembled monolayers of thiolates on metals as a form of nanotechnology. *Chemical Reviews*, *105*(4), 1103–1169). doi:10.1021/cr0300789

J.R. Macdonald (1948), Note on the parameterization of the constant-phase admittance element, *Solid State Ionics, 13*, 147-149

Ma, W., Yin, H., Xu, L., Wu, X., Kuang, H., Wang, L., & Xu, C. (2014). Ultrasensitive aptamer-based SERS detection of PSAs by heterogeneous satellite nanoassemblies. *Chemical Communications, 50*, 9737-9740. doi:10.1039/c4cc03734k

McKeague, M., Giamberardino, A., & DeRosa, M. C. (2011). Advances in aptamer-based biosensors for food safety. In *Environmental Biosensors* (Somerset, V., ed.), InTech, pp. 17-42. doi:10.5772/22350

O'Sullivan, C. K., & Guilbault, G. G. (1999). Commercial quartz crystal microbalances – theory and applications. *Biosensors and Bioelectronics, 14*(8-9), 663–670. doi:10.1016/S0956-5663(99)00040-8

Pestourie, C., Cerchia, L., Gombert, K., Aissouni, Y., Boulay, J., De Franciscis, V., Libri, D., Tavitian, B. & Ducongé, F. (2006). Comparison of different strategies to select aptamers against a transmembrane protein target. *Oligonucleotides, 16*(4), 323-335. doi:10.1089/oli.2006.16.323

Radi, A. E., & O'Sullivan, C. K. (2006). Aptamer conformational switch as sensitive electrochemical biosensor for potassium ion recognition. *Chemical Communications*, 3432-3434. doi:10.1039/b606804a

Rodriguez, M.C., Kawde, A.N., & Wang, J., (2005). Aptamer biosensor for label-free impedance spectroscopy detection of proteins based on recognition-induced switching of the surface charge. *Chemical Communications(34),* 4267-4269. doi: 10.1039/B506571B

Savory, N., Abe, K., Sode, K., & Ikebukuro, K. (2010). Selection of DNA aptamer against prostate specific antigen using a genetic algorithm and application to sensing. *Biosensors and Bioelectronics, 26*(4), 1386–1391. doi:10.1016/j.bios.2010.07.057

Song, S., Wang, L., Li, J., Fan, C., & Zhao, J. (2008). Aptamer-based biosensors. *Trends in Analytical Chemistry, 27*(2), 108–117. doi:10.1016/j.trac.2007.12.004

Steel, A. B., Herne, T. M., & Tarlov, M. J. (1998). Electrochemical quantitation of DNA immobilized on gold. *Analytical Chemistry, 70*(22), 4670–4677. doi: 10.1021/ac980037q

Stoltenburg, R., Reinemann, C., & Strehlitz, B. (2007). SELEX—a (r)evolutionary method to generate high-affinity nucleic acid ligands. *Biomolecular Engineering, 24*(4), 381-403. doi:10.1016/j.bioeng.2007.06.001

Voinova, M. V, Rodahl, M., Jonson, M., & Kasemo, B. (1999). Viscoelastic acoustic response of layered polymer films at fluid-solid interfaces: continuum mechanics approach. *Physica Scripta*, *59*(5), 391–3. doi:10.1238/Physica.Regular.059a00391

Zhang, W.M., Leinonen, J., KalkKinen, N., Dowell, B., & Stenman, U.H. (1995). Purification and characterization of different molecular forms of prostate-specific antigen in human seminal fluid. *Clinical Chemistry, 41*(11), 1567-1573.

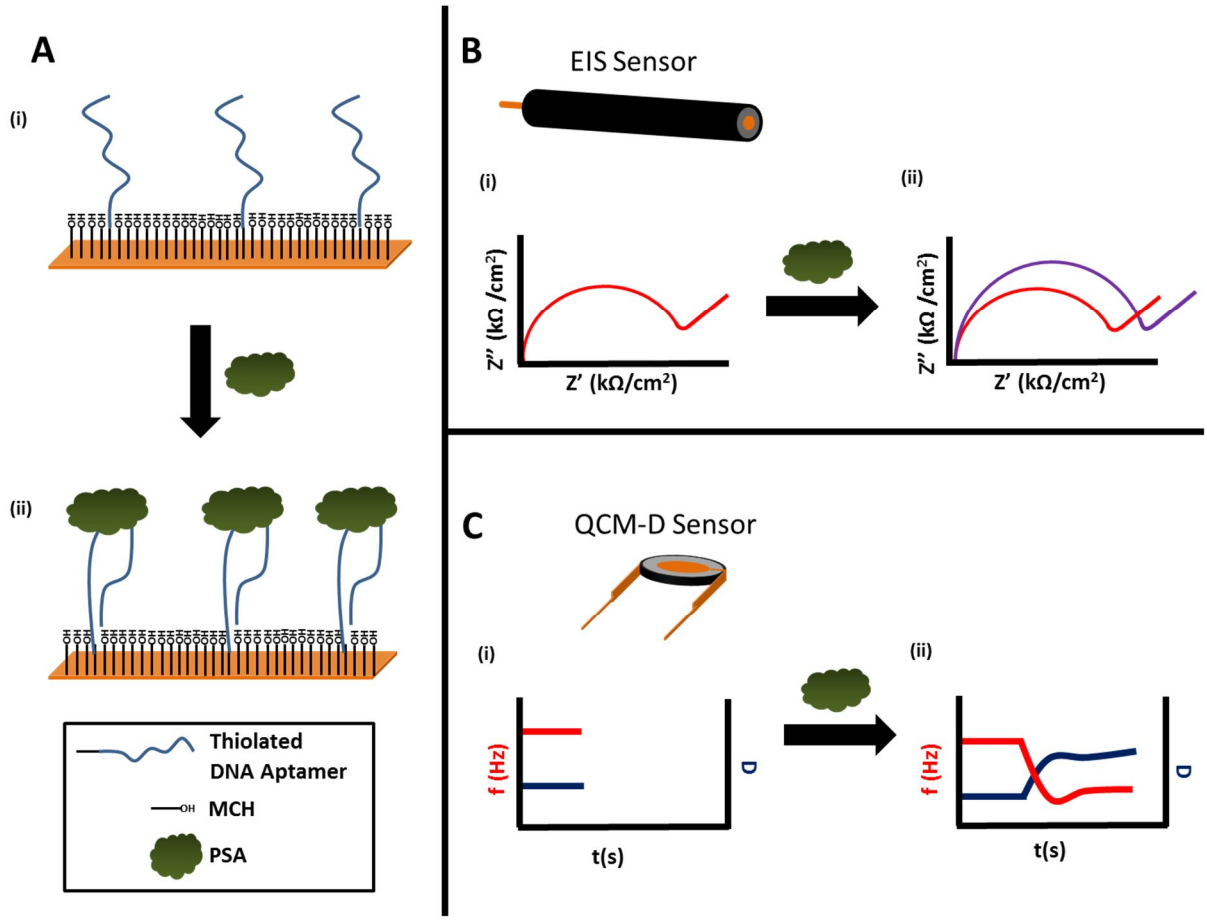

Fig.1. A) Biosensor detection principle with representation of the electrode gold surface; **B)** EIS measurements showing a signal change in the Nyquist plot before **(i)** and after **(ii)** PSA binding; **C)** QCM-D measurements showing frequency and dissipation responses before **(i)** and after **(ii)** PSA binding.

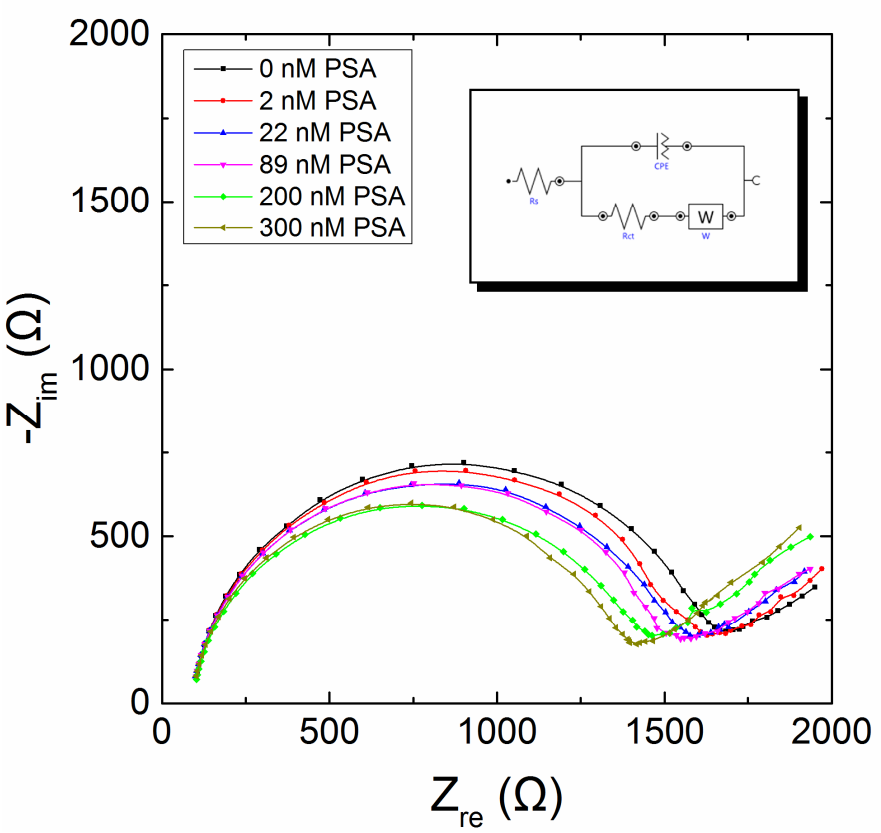

Fig.2. Nyquist plot for different PSA concentrations using an aptamer/MCH ratio of 1:100. Inset: Randles equivalent circuit. R_s is the solution resistance, R_{ct} is the charge transfer resistance, CPE is the constant phase element and W is the Warburg element.

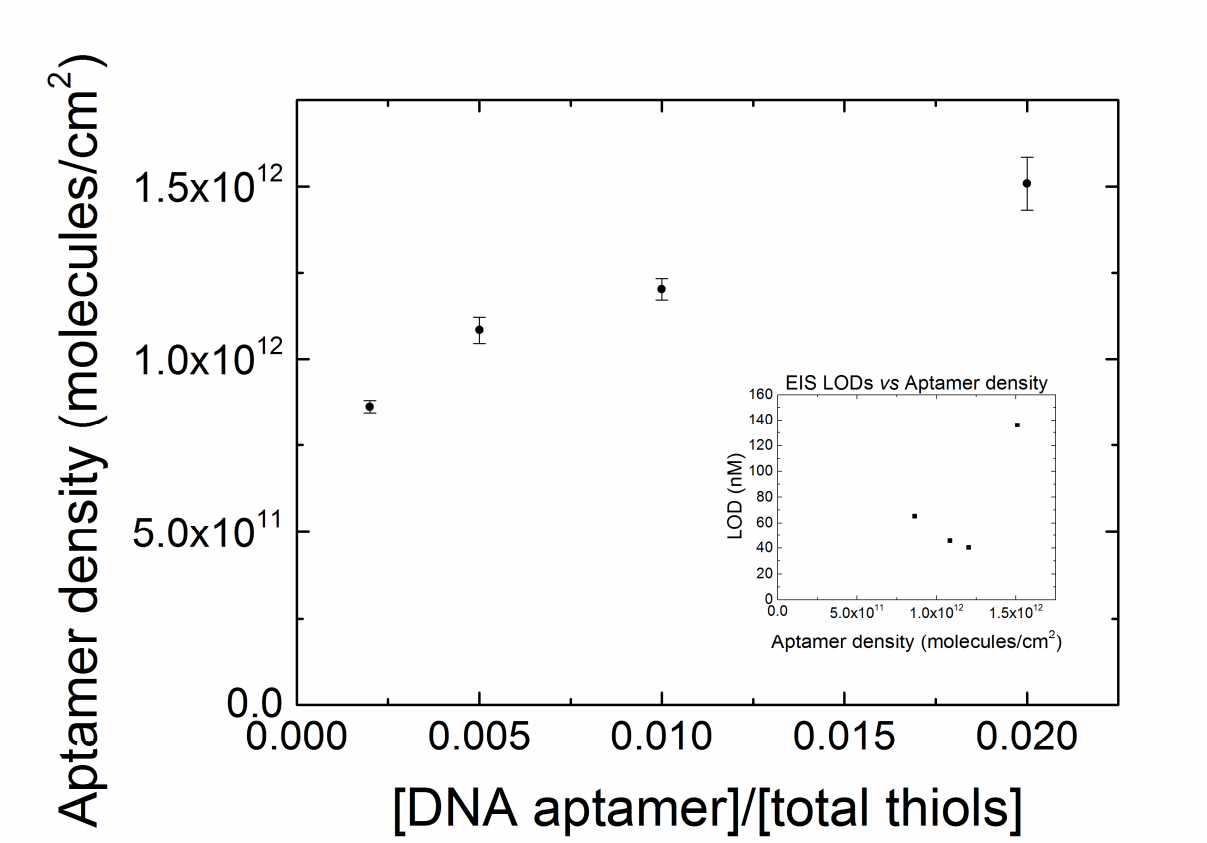

Fig. 3. DNA aptamer molecule density distribution on the electrode surface *vs.* DNA aptamer/MCH molar fraction in solution. Active electrode surface: 1 mm radius. Inset: LODs obtained from the EIS responses for different DNA aptamer/MCH molar fraction *vs.* surface aptamer density

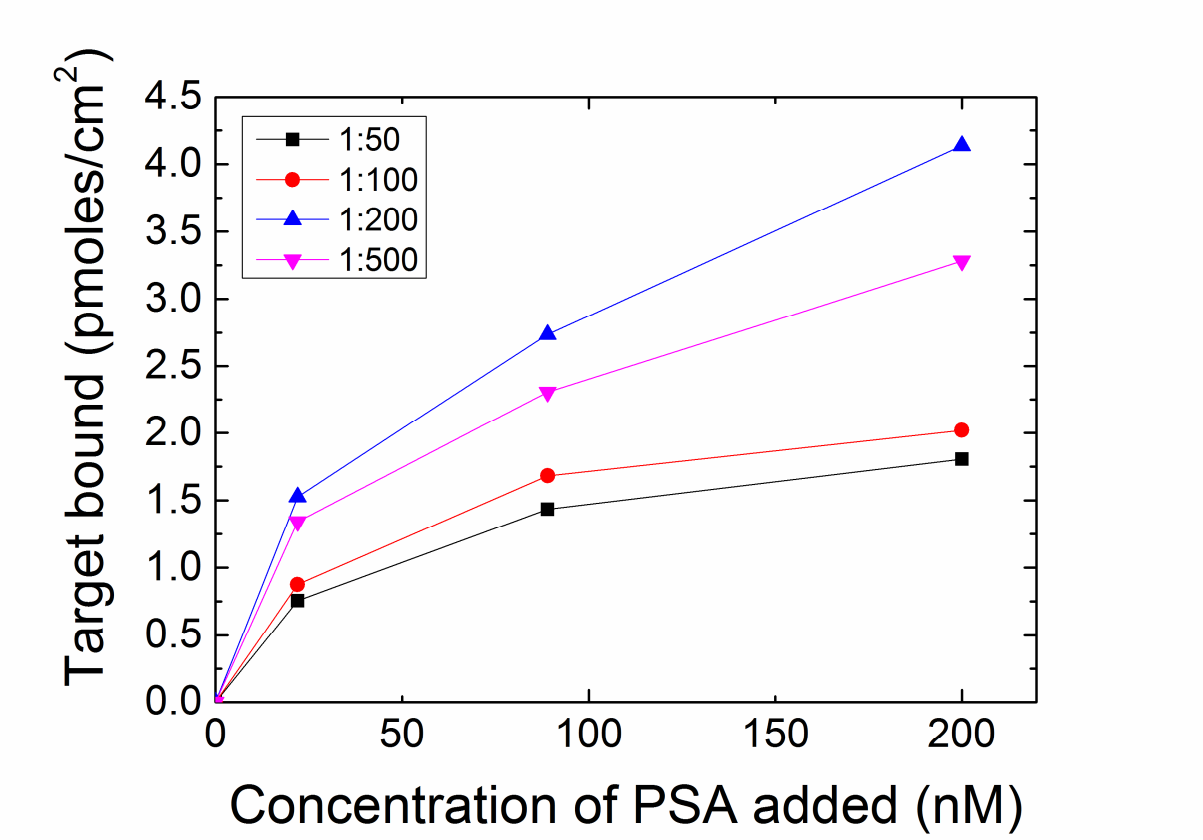

Fig. 4. Hydrated mass QCM-D measurements in a flow mode for PSA binding at different DNA aptamer/MCH ratios.

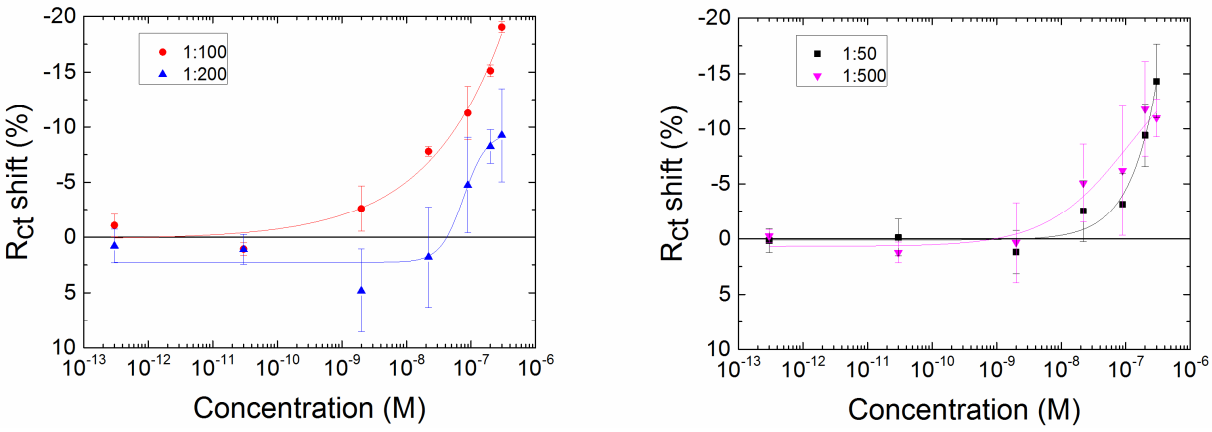

Fig. 5. R_{ct} change upon incubation with PSA in different SAM over range of DNA aptamer/MCH concentration fraction. The lines, which serve as guides to the eye, are fits of the data to a Hill dose response equation: $y = y_0 + (y_{max} - y_0)\, c^n / (k^n + c^n)$ where c is the concentration.

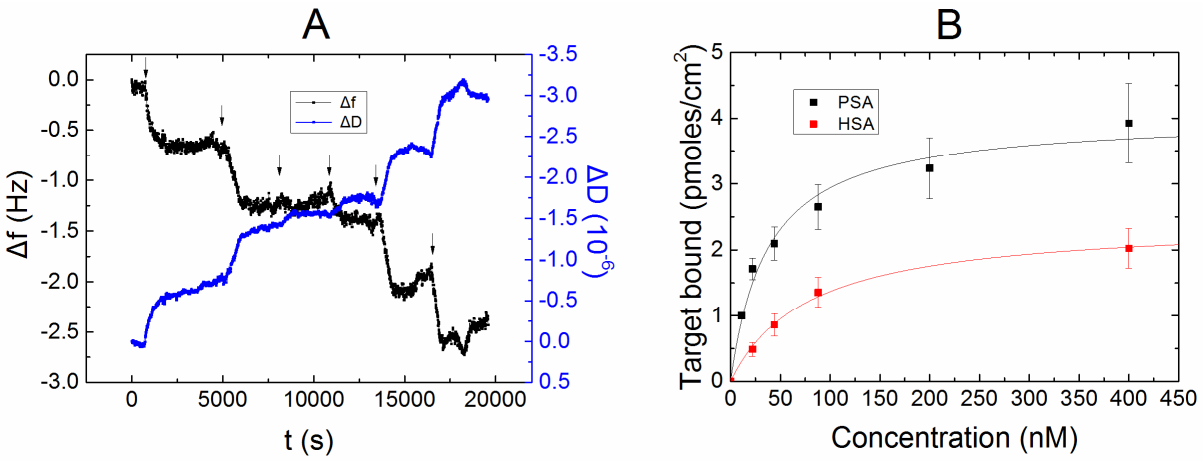

Fig. 6. A) Kinetic curves of frequency and dissipation response upon increasing PSA additions in flow-condition. Arrows indicate additions of PSA; **B)** Hydrated mass QCM-D response in a flow mode for PSA and HSA using an aptamer/MCH ratio of 1:200. Fitting is obtained by using a hyperbolic dose response equation $y = y_{max}\, c/(K_d + c)$ where c is the concentration and K_d the affinity constant